Journal of Materials Research and Technology 28 (2024) 1013–1021

Contents lists available at ScienceDirect

Journal of Materials Research and Technology

journal homepage: www.elsevier.com/locate/jmrt

First-principles analysis of the effects of oxygen, vacancies, and their complexes on the screw dislocation motion in body-centered cubic Nb

Tomohito Tsuru [a,b,c,*], Ivan Lobzenko [a], Shigenobu Ogata [d,b], Wei-Zhong Han [e]

[a] Nuclear Science and Engineering Center, Japan Atomic Energy Agency, 2-4 Shirakata, Tokai-mura, Ibaraki, 319-1195, Japan
[b] Center for the Promotion of Interdisciplinary Education and Research, ESISM, Kyoto University, Yoshida, Honmachi, Sakyo-ku, Kyoto, 606-8501, Japan
[c] PRESTO, Japan Science and Technology Agency, 4-1-8 Honcho, Kawaguchi, Saitama, 332-0012, Japan
[d] Department of Mechanical Science and Bioengineering, Osaka University, 1-3 Machikaneyama, Toyonaka, Osaka, 560-8531, Japan
[e] Center for Advancing Materials Performance from the Nanoscale (CAMP-Nano), State Key Laboratory for Mechanical Behavior of Materials, Xi'an Jiaotong University, Xi'an, 710049, China

ARTICLE INFO

Key workds:
Strengthening
Dislocation
Oxygen
Body-centered cubic Nb
First-principles

ABSTRACT

Some solute atoms induce strengthening and embrittlement in body-centered cubic refractory metals. Especially, interstitial oxygen produces remarkable strengthening effects in Nb, wherein the yield stress of oxygen-doped Nb alloys is more than twice that of pure Nb. Conventional mechanisms cannot explain this oxygen-induced dramatic strengthening because the interaction between dislocations and oxygen atoms is not so significant. In a previous study, we found that the formation of vacancy–oxygen pairs enhances the attractive interaction with a screw dislocation and increases the energy barrier for dislocation motion associated with cross-kink nucleation in Nb–O alloys. However, the strengthening effect could not be described by the pinning model for dislocation motion. Herein, we focused on the atomic-level analysis of the fundamental process related to the dislocation motion around a vacancy, an oxygen atom, and a vacancy–oxygen pair. First-principles calculations revealed that the vacancy–oxygen pairs increase the energy barrier with respect to the dislocation motion more substantially than vacancies and oxygen interstitials owing to a unique oxygen-induced mechanism; an octahedral–tetrahedral shuffling process of oxygen is necessary for dislocation passing through vacancy–oxygen obstacles. Such event almost never happens in the real metallic materials. Instead, cross-kink nucleation occurs frequently to overcome the widely distributed vacancy–oxygen obstacles, which contributes to the dramatic strengthening.

1. Introduction

Some early transition body-centered-cubic (BCC) metals have been used for developing nuclear structural materials, casting molds, and other practical applications in refractory metals [1,2]. These metals usually exhibit excellent high-temperature strength. However, the mechanical properties of these metals deteriorate rapidly in the presence of diluted impurities such as oxygen (O), carbon (C), and nitrogen (N) [3–9]. The oxygen concentration in these metals needs to be carefully monitored because oxygen in the air tends to dissolve easily into the matrix during processing or service [2–5]. For example, O atoms are highly soluble in niobium (Nb), leading to strengthening and embrittlement even at low concentrations [10]. The resulting deterioration in the deformability and fracture toughness of Nb hinders the use of Nb in a wide range of applications. Solid-solution strengthening has conventionally been attributed to the interaction between solute atoms and dislocation cores [11–17]. The formation of a Cottrell atmosphere involving interstitial solutes, causing the pinning effect for the dislocation motion, results in a potential strengthening mechanism in BCC alloys. However, this mechanism cannot be used to explain the dramatic increase in the yield stress observed in oxygen-doped Nb alloys.

Another potential strengthening mechanism is the pinning of screw dislocations. Density functional theory (DFT) calculations showed that interstitial atoms like carbon and hydrogen often create specific interactions other than elastic interactions with a screw dislocation [18–22]. For example, an intermediate atomic configuration forms during the motion of a screw dislocation, which is similar to that of the stable carbide, resulting in a strong attractive interaction with the carbon in iron [18]. However, a study by Lüthi [20] and our preliminary first-principles calculations showed that this mechanism is not

* Corresponding author. Nuclear Science and Engineering Center, Japan Atomic Energy Agency, 2-4 Shirakata, Tokai-mura, Ibaraki 319-1195, Japan.
E-mail address: tsuru.tomohito@jaea.go.jp (T. Tsuru).

https://doi.org/10.1016/j.jmrt.2023.12.033
Received 2 November 2023; Received in revised form 1 December 2023; Accepted 4 December 2023
Available online 9 December 2023

applicable to oxygen interstitials in Nb. We recently demonstrated that screw dislocations moving through a random repulsive force field generated by oxygen interstitial impurities readily form cross-kinks and emit excess vacancies in Nb [10]. These vacancies bind strongly with oxygen and screw dislocation in a three-body manner, hindering dislocation motion and resulting in pronounced dislocation storage and strengthening. Interestingly, the yield stress of oxygen-doped Nb alloys is more than twice that of pure Nb. The three-body (vacancy–oxygen–dislocation) interaction plays an essential role in the strengthening of oxygen-doped Nb alloys.

Our previous calculations indicated that the strongly attractive interaction between the vacancy–oxygen pair and a screw dislocation increases the energy barrier for the dislocation motion, and subsequent frequent cross-kink nucleation contributes to the accumulation of damage [10]. However, an unresolved question is why the energy barrier for the dislocation motion is considerably higher for a vacancy–oxygen pair than for an isolated vacancy and an oxygen interstitial. In this study, we investigated the atomic-level mechanism underlying the three-body interaction involving a screw dislocation, vacancy, and an oxygen interstitial as the predominant strengthening mechanism in oxygen-doped Nb alloys. We performed first-principles calculations on a dislocation core structure and explored the fundamental interaction process to elucidate the strengthening mechanism.

2. Simulation methods

In this study, we performed first-principles calculations to investigate the effect of an oxygen interstitial on the motion of a screw dislocation. We first constructed atomic models of the dislocation core structure. A dislocation dipole with quadrupolar configuration was incorporated into a periodic cell using a solution to realize a periodic dislocation dipole array based on continuum linear elasticity theory [23]. We performed preliminary calculations to determine the fundamental material properties of Nb and confirmed the values were consistent with other calculations [24]. The lattice constant was found to be $a_0 = 3.323$ Å, and the elastic constants needed to solve the elastic problem related to dislocation dipole were found to be $c_{11} = 254.2$, $c_{12} = 135.4$, and $c_{44} = 19.9$ GPa. The distortion field of the dislocation quadrupole array was then selected to minimize the total elastic energy under the topological constraints imposed owing to screw dislocation. The displacement field was calculated by performing line integrals [23] and used for the initial atomic position of the dislocation dipole [25,26]. A <111> screw dislocation dipole was considered in this study. As shown in Fig. 1 (a), a dislocation dipole was inserted into a 135-atom supercell having the following dimensions: $\mathbf{a} = 5\mathbf{e}_1'$, $\mathbf{b} = 2.5\mathbf{e}_1' + 4.5\mathbf{e}_2'$, and $\mathbf{c} = \mathbf{e}_3'$, where $\mathbf{e}_1'$, $\mathbf{e}_2'$, and $\mathbf{e}_3'$ are defined as $a_0[\sqrt{6}, 0, 0]$, $a_0[0, \sqrt{2}, 0]$, and $a_0[0, 0, \sqrt{3}/2]$ along $x = [11\bar{2}]$, $y = [1\bar{1}0]$, and $z = [111]$, respectively. The positions of the atoms in the supercell were based on the BCC crystal coordinate system. The elastic field related to dislocations under a periodic boundary condition can be constructed by superimposing the field produced in the simulation cell on the image field of its periodic replica; however, the system energy may be conditionally convergent [27,28]. Changes in the relative positions of dislocation dipoles in a periodic cell increase the effect of the image field. This effect cannot be neglected for small supercells. In this study, we examined the energy barrier for the dislocation motion in Nb alloys, where both dipole dislocations were considered to move in the case of pure Nb and only one dislocation of the dipole was considered to move in other cases. We used the linear elasticity theory to estimate the pseudoenergy needed to realize a change in the relative position of two dislocations [23]. The elastic solution for a periodic array of dislocation dipoles in an isotropic medium was determined in a reciprocal space using a dislocation core radius of $b/4$ and a smearing factor to treat the singularity. Fig. 1 (b) shows the relationship between the dipole energy and relative dipole position for the periodic cell used in the first-principles calculations,

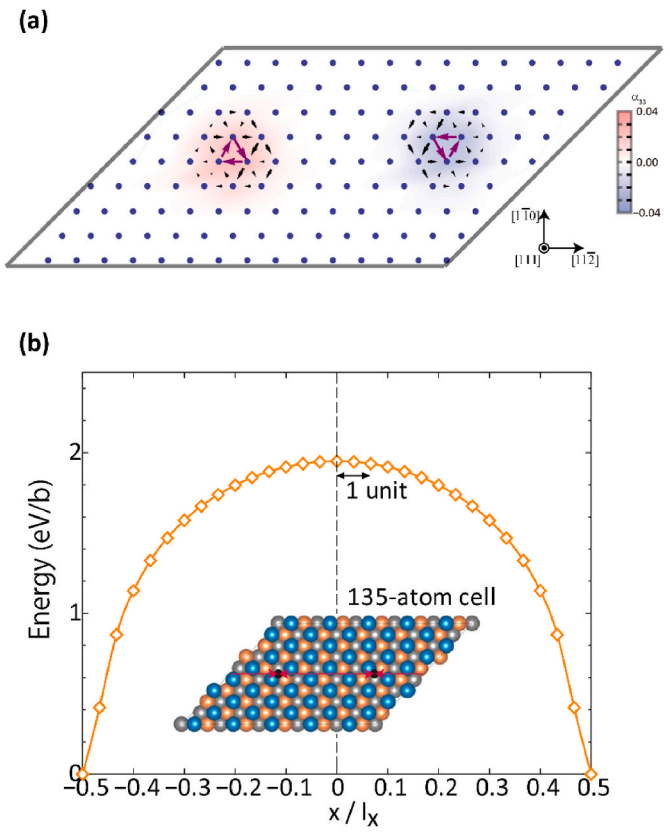

Fig. 1. The core structure and energy of a screw dislocation dipole in a periodic cell. (a) Dislocation dipole in a 135-atom supercell visualized by the DD vector and Nye tensor. (b) The relationship between the dipole energy and the change in the relative position of dislocations evaluated using elasticity theory.

where $x/l_x = 0$ corresponds to the equilibrium quadrupolar configuration. The pseudoenergy related to the dislocation moving on one side of a lattice is 16 meV/b. This estimate based on elasticity theory is in good agreement with the result of the first-principles calculation (18.2 meV/b). Energy calibration in cases of pure BCC metals can be effectively performed using the estimate based on elastic theory; however, this calibration remains challenging for complex alloy systems. This dislocation dipole model decreased the size dependence of the dislocation core energy [29,30]. The dislocation core structure and the Peierls potential related to the dynamic behavior of dislocations, such as the enthalpy of kink formation and non-Schmid behavior, were determined with sufficient accuracy [31,32]. Thus, we selected a three-layer supercell model along the <111> direction comprising 405 atoms. We employed the Aneto software proposed by Clouet et al. [33] to evaluate the relationship between the energy obtained when a vacancy is embedded in periodic cells and the true energy of an isolated vacancy in infinite media, and calculated the energy correction. We calculated an energy correction of 2.6 meV using the following inputs for the case of vacancies. Given the relatively large size of the supercell, first-principles calculations using the supercell can yield a sufficiently accurate energy value for an isolated point defect.

First-principles calculations were carried out within the DFT framework to obtain a stable configuration of a dislocation core around a vacancy and an oxygen interstitial. The interaction energy between these defects was then calculated. The DFT calculations were implemented using the Vienna ab initio simulation package (VASP) [34,35] with the Perdew–Burke–Ernzerhof formulation of the generalized gradient approximation to the exchange-correlation density functional [36]. A cutoff energy of the plane wave of 400 eV was applied in conjunction with the first-order Methfessel–Paxton scheme and a

smearing parameter of 0.1 eV. Brillouin-zone k-point samplings were selected using the Monkhorst–Pack algorithm [37]. All calculations were performed using $1 \times 1 \times 6$ k-point sampling. The self-consistent field calculations converged for an energy difference below 10^{-5} eV. The conjugate gradient method was used to determine the fully relaxed configurations, where the search was terminated when the force on all the atoms decreased to below 0.01 eV/Å. The nudged elastic band (NEB) method was used to calculate the transition states that formed during dislocation motion [38]. Nine intermediate replica images were used in the NEB simulation, and the convergence condition was that the forces were below 0.03 eV/Å. The atomic model used in this study was visualized using VESTA [39] software and our dislocation core analyzer. Fig. 1 (a) shows the relaxed dislocation core structure in Nb calculated by DFT and visualized using the differential displacement (DD) vector [40] and Nye tensor [41]. This dislocation model in pure Nb was used as the reference configuration for further analysis.

3. Results and discussion

3.1. Two-body interactions between defects and oxygen

First, we performed DFT calculations to investigate the two-body interaction between defect structures in Nb. In the previous study, we studied the two-body interaction involving oxygen [10]. In this study, we considered two-body interactions involving other interstitial elements such as C and N. The interaction energies are defined as following relations:

$$E_{\mathrm{int}}^{\mathrm{V-I}} = \left(E^{\mathrm{V-I}} + E^{\mathrm{pure}}\right) - \left(E^{\mathrm{V}} + E^{\mathrm{I}}\right), \tag{1}$$

$$E_{\mathrm{int}}^{\mathrm{SC-V}} = \left(E^{\mathrm{SC-V}} + E^{\mathrm{pure}}\right) - \left(E^{\mathrm{SC}} + E^{\mathrm{V}}\right), \tag{2}$$

$$E_{\mathrm{int}}^{\mathrm{SC-I}} = \left(E^{\mathrm{SC-I}} + E^{\mathrm{pure}}\right) - \left(E^{\mathrm{SC}} + E^{\mathrm{I}}\right), \tag{3}$$

where the energyies $E^{\mathrm{V-I}}$, E^{V}, E^{I}, and E^{pure} are the total energy of structures including vacancy-interstital pair, a vacancy, an interstital, and defect-free crystal, respectively. Fig. 2 shows the two-body interaction energies within third nearest neighbor (NN) configurations considering C, N, and O as the interstitials: (i) a vacancy–interstitial pair in a perfect crystal, (ii) a screw dislocation–vacancy pair, and (iii) a screw dislocation–interstitial pair. Fig. 2 (a) shows the apparent differences and trends related to the (i) vacancy–interstitial interaction involving different interstitials. Oxygen interstitials have a stronger attractive interaction with a vacancy than other interstitials in the Nb matrix. The interaction energies of the vacancy–oxygen pair are −0.80, −0.17, and 0.13 eV for the first to third NN configurations. Fig. 2 (b) shows the two-body interaction energies of the (ii) dislocation–vacancy

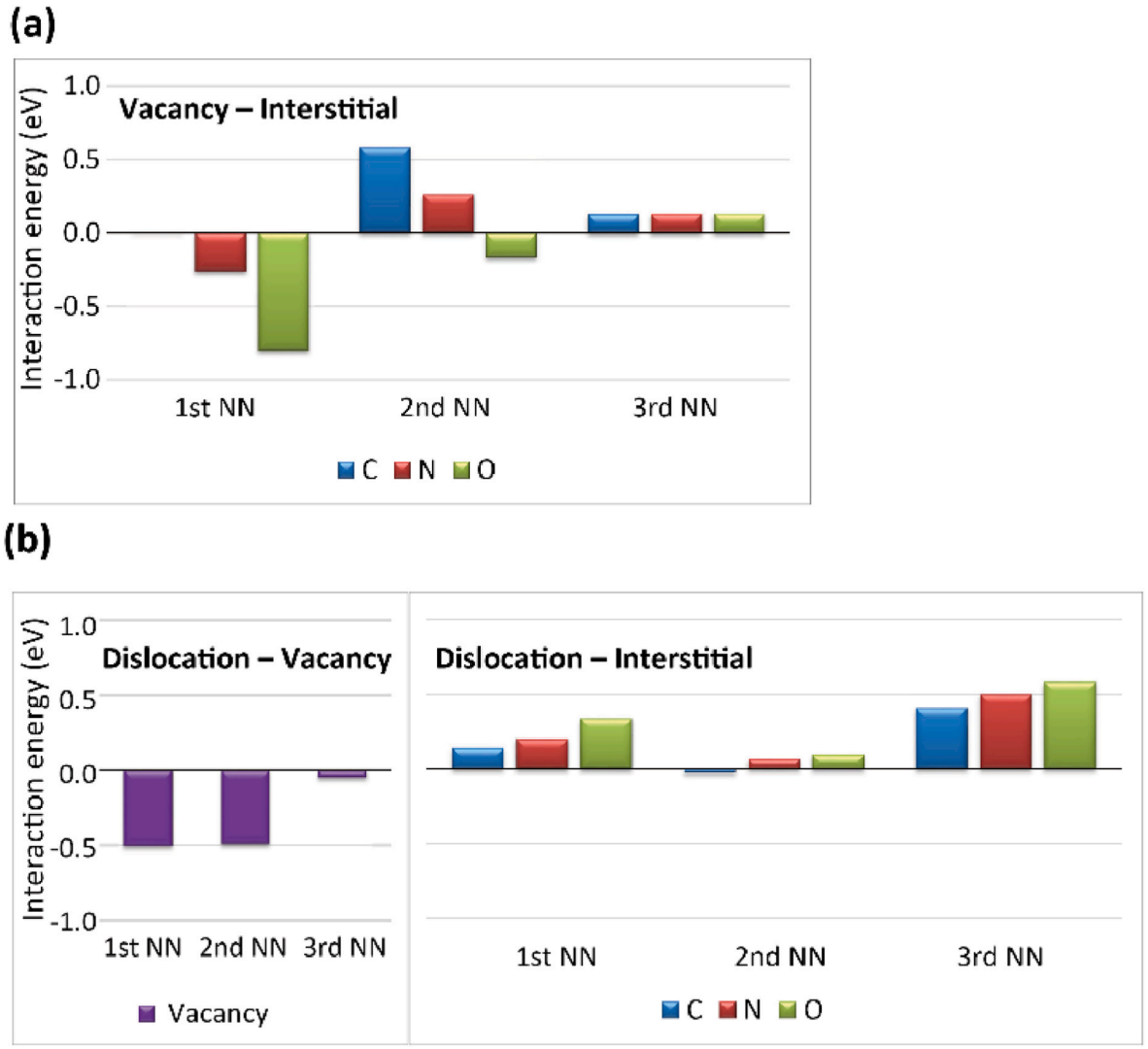

Fig. 2. Two-body interactions for vacancy–interstitial, screw dislocation–vacancy and screw dislocation–interstitial combinations. (a) The interaction energy of vacancy–interstitial (C, N, and O) pairs in a perfect crystal. (b) The interaction energy among a screw dislocation, vacancy, and an interstitial (C, N, and O).

and (iii) dislocation–interstitial.

The interaction energies between a screw dislocation and a vacancy for the first, second, and third NN configurations are −0.51, −0.49, and −0.051 eV, respectively. A strong attractive interaction exists between a vacancy and a screw dislocation; however, this attraction is extremely short-ranged and dominant only within the second NN configuration. The interaction between a screw dislocation and interstitials is repulsive in most cases. In particular, the repulsive interaction of dislocation–oxygen is stronger than that of dislocation–carbon and dislocation–nitrogen. The interaction energies of dislocation–oxygen for the first, second, and third NN configurations being 0.34, 0.086, and 0.55 eV, respectively. Our preliminary calculations showed that an extremely large repulsive interaction is generated when an interstitial is placed in the center of the dislocation core. These results indicate that interstitial solutes do not segregate around screw dislocations. We investigated how an oxygen interstitial behaves and influences dislocation motion in the Nb matrix. This repulsive interaction is caused by the electronic structures of Nb and oxygen around the dislocation core. The oxygen atoms weaken the bond between the core and Nb by decreasing the number of electronic states below the Fermi level, and this effect is strongest near the dislocation core. Our preliminary calculations also showed that the presence of an oxygen interstitial decreases the charge density in the easy and hard-core configurations. This result indicates that Nb atoms in the vicinity of a dislocation core form unstable bonds with oxygen in all cases. The existence of a repulsive interaction between dislocations and oxygen interstitials contradicts the experimental observations based on a three-dimensional atom probe analysis indicating that oxygen and other interstitial solutes tend to aggregate along the dislocation line [10]. Our interest is why oxygen atoms are trapped around dislocation despite the repulsive interaction.

3.2. Three-body interaction between defects and oxygen

A possible strengthening mechanism is created during a three-body interaction involving a dislocation and vacancy–oxygen interstitial. In addition to the results discussed in a previous study [10], we investigated the interactions with respect to various three-body configurations. In this study, the energy of a three-body interaction is defined as the energy related to the interaction between a vacancy–oxygen pair and a screw dislocation as following relation.

$$E_{\mathrm{int}}^{\mathrm{SC-(V-I)}} = \left(E^{\mathrm{SC-(V-I)}} + E^{\mathrm{pure}}\right) - \left(E^{\mathrm{SC}} + E^{\mathrm{V-I}}\right), \tag{4}$$

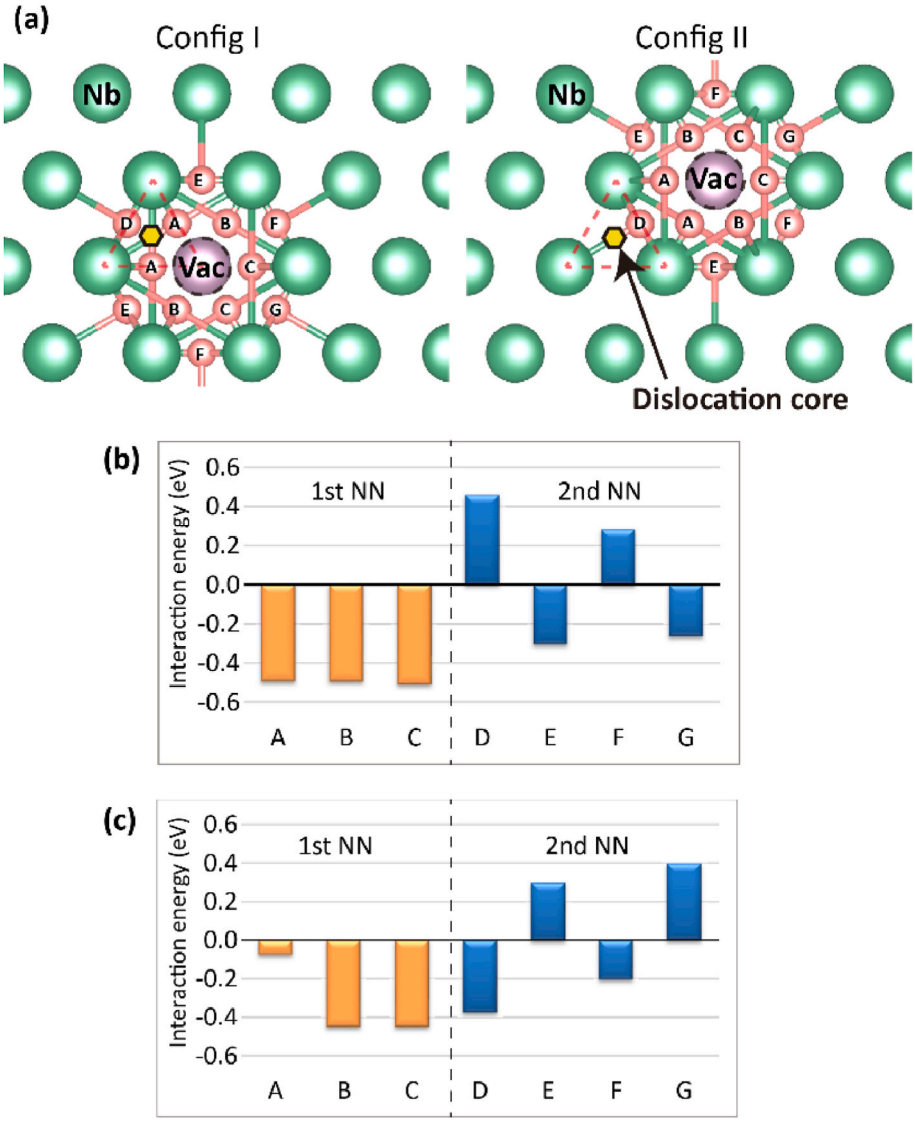

Fig. 3. Three-body interactions between a screw dislocation and a vacancy–oxygen complex. (a) Atomic configurations of various oxygen interstitial sites (A–G) for vacancies at the first and second NN configurations of a screw dislocation (Config I and Config II, respectively). (b) The interaction energy for Config I. (c) Same as (b), but for Config II.

where $E^{SC-(V-I)}$ is the total energy of the stucutre corresponding to Fig. 3 (a). Interstitial solutes generally anneal rapidly during plastic flow because of high solute diffusivity, which does not influence the strengthening process. However, stable vacancy–oxygen pairs disperse widely in a matrix owing to the interactions between vacancies and oxygen interstitials. These stable complexes can present strong obstacles to dislocation motion. Therefore, we evaluated the three-body interaction around a dislocation. The strongest attractive interaction between a dislocation and vacancy occurs when the vacancy is located at the first NN site from the dislocation core. We used the most stable configuration of the two-body interaction to assess a three-body interaction between a vacancy–oxygen pair and a screw dislocation. We constructed atomic models by inserting an oxygen interstitial into the relaxed configuration of a dislocation core having a vacancy model. The initial configuration is shown in Fig. 3 (a), where A, B, C, …, and G indicate equivalent interstitial sites around a dislocation and a vacancy. The A–C and D–G sites correspond to the first and second NN configurations in terms of the vacancy positions. Each mark indicates the same position relative to the vacancy around the dislocation core. The interaction energy of this three-body configuration was defined as the difference between the energies of the above-mentioned configuration and the isolated defect configuration. The interaction energy is shown in Fig. 3 (b). The interaction between a vacancy–oxygen pair and screw dislocation is attractive when the vacancy is in the vicinity of the dislocation core. The interaction energy of the most stable configuration is −0.5 eV. The results of DFT calculations for the two- and three-body interactions show an attractive interaction between oxygen interstitials and vacancies, resulting in a strong attractive interaction between a vacancy–oxygen pair and screw dislocation. However, this attractive interaction is similar to that between dislocations and mono vacancy.

We utilized the results of the DFT calculation presented above to infer the underlying mechanism of the dramatic strengthening observed in Nb–O. First, we estimated the contribution to strengthening from pinning induced by the attractive interaction between a vacancy or a vacancy–oxygen pair and screw dislocations. As discussed above, the interaction between a dislocation and a vacancy–oxygen pair calculated by DFT is $E_i = -0.5$ eV. Assuming that vacancies are distributed homogeneously with an equilibrium concentration (~10 ppm [42,43]), the increment in the yield stress caused by the attractive interaction was estimated to be 35.5 MPa. The attractive interaction certainly contributes to the strengthening; however, we confirmed that the contribution is insignificant compared with actual experimental results, which cannot explain the dramatic strengthening observed in the experiments. Therefore, a detailed investigation of the dislocation migration process other than interaction energy should be considered to understand the unique phenomenon caused by the three-body interaction.

3.3. Energy barrier for the dislocation motion around defect complexes

We consider the effect of a vacancy, oxygen, and a vacancy–oxygen pair on dislocation motion. We performed NEB simulations to evaluate the energy barrier for the dislocation motion around a vacancy, an oxygen interstitial, and an oxygen–vacancy pair. As for pure Nb, the migration energy of a screw dislocation is 0.03 eV/b. It is difficult to evaluate the length-independent interaction energy between a dislocation and obstacles and the length-dependent migration energy. Therefore, we attempted to evaluate the relative contributions using normalized values such as the energy barrier per unit length for the case of various obstacles per 3b length. Fig. 4 (a) shows the atomic configurations for the dislocation core in the vicinity of a vacancy. Fig. 4 (b)

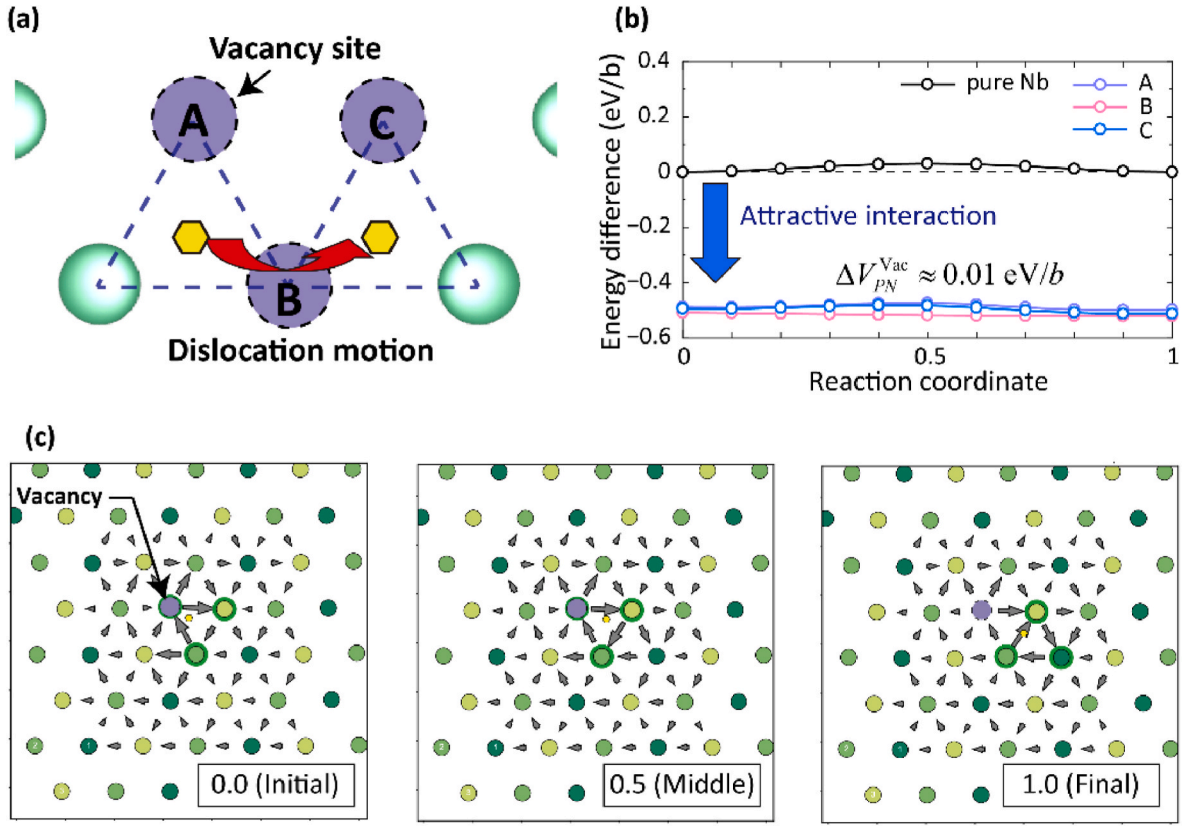

Fig. 4. Energy barrier and core configuration related to dislocation motion around a vacancy. (a) Schematic of the relative configurations for three vacancy sites along the migration path of a dislocation core. (b) The change in energy during the motion of a screw dislocation around a vacancy. (c) The change in the configuration of a dislocation core around a vacancy at Site A, as visualized by the DD vector, where the position of Nb along the <111> direction is shown in colors ranging from dark to light green.

shows the change in the energy during dislocation motion around a vacancy and Fig. 4 (c) shows the change in the configuration of the dislocation core around a vacancy at Site A during dislocation motion, as visualized by the DD vector. The position of the dislocation core is located within three atomic rows with large displacement components along the direction of the Burgers vector. A one-to-one relationship between the displacement components of the three atomic rows and the two-dimensional position perpendicular to the Burgers vector has been identified in pure BCC metals [44]. In this study, we used this relationship to predict the position of the dislocation core based on only the displacement components of the Nb atoms, as indicated by the yellow dots in the DD vector images shown in Fig. 4 (c) and similar figures shown later. As discussed above, a strong attractive interaction exists between a screw dislocation and a vacancy. The energy barrier corresponding to this attractive interaction must be overcome for a dislocation to glide, showing that a vacancy presents a strong obstacle to a dislocation moving away from the vacancy. However, the difference in the energies of the initial and saddle-point configurations is on the order of 0.01 eV/b and not very large. Note that if the relative positions of the dislocation and vacancy are away from 2NN, 0.5 eV corresponding to the interaction energy is added to the energy barrier. Therefore, a vacancy in Nb simply contributes to the strengthening via the attractive interaction with screw dislocations.

The energy barrier for the dislocation motion through an oxygen interstitial was similarly examined. Fig. 5 (a) and (b) show the atomic configuration and the change in energy for dislocation motion with oxygen at the 1st NN site, respectively. Fig. 5 (c) shows the change in the configuration of the dislocation core around oxygen at Site B during dislocation motion. The energy barrier tends to increase slightly and oxygen is pushed away by the repulsive interaction during the approach of the dislocation core. By contrast, the energy barrier decreases when the dislocation moves away from the oxygen. In this case, the maximum Peierls barrier is 0.08 eV/b.

Finally, we consider the effect of the three-body interaction on dislocation motion. Fig. 6 (a) and (b) show the two configurations with different positions relative to the dislocation motion and the vacancy taken as references. An oxygen interstitial was inserted into the most stable site obtained for each configuration, as shown in Fig. 3. NEB simulations were performed to determine the energy barrier for the dislocation motion around the vacancy–oxygen pair. Fig. 6 (c) and (d) show the change in the energy during the motion of the screw dislocation around the vacancy–oxygen pair, where the energy of a dislocation–vacancy–oxygen three-body complex is defined as the difference in the energies between the isolated dislocation and vacancy–oxygen pair in the perfect crystal. Considering the energy of the initial configuration, the interaction between the dislocation and vacancy–oxygen pair is attractive ($E_i = -0.5$ eV). A dislocation must overcome this high-energy barrier to move away from the vacancy–oxygen pair. There is an exceedingly high-energy barrier for a dislocation to move across the stable vacancy–oxygen pair (Configs. II-B and II-C), which cannot be explained in terms of simple attraction or repulsion, as discussed later.

We focused on the configurational change of the dislocation and oxygen corresponding to Config II-B. Fig. 7 (a) and (b) show the minimum energy path and local configuration of the dislocation core during dislocation motion between several local minima. Unlike the results for the isolated oxygen interstitial, oxygen appears to move during the dislocation motion. Fig. 7 (a) shows a double-humped energy barrier from 0.0 to 1.0, and the corresponding change in the oxygen position is shown in Fig. 7 (c). The oxygen is accompanied by a significant motion when the dislocation moves across in-between vacancy and oxygen within a pair. This process is similar to that observed in titanium–oxygen

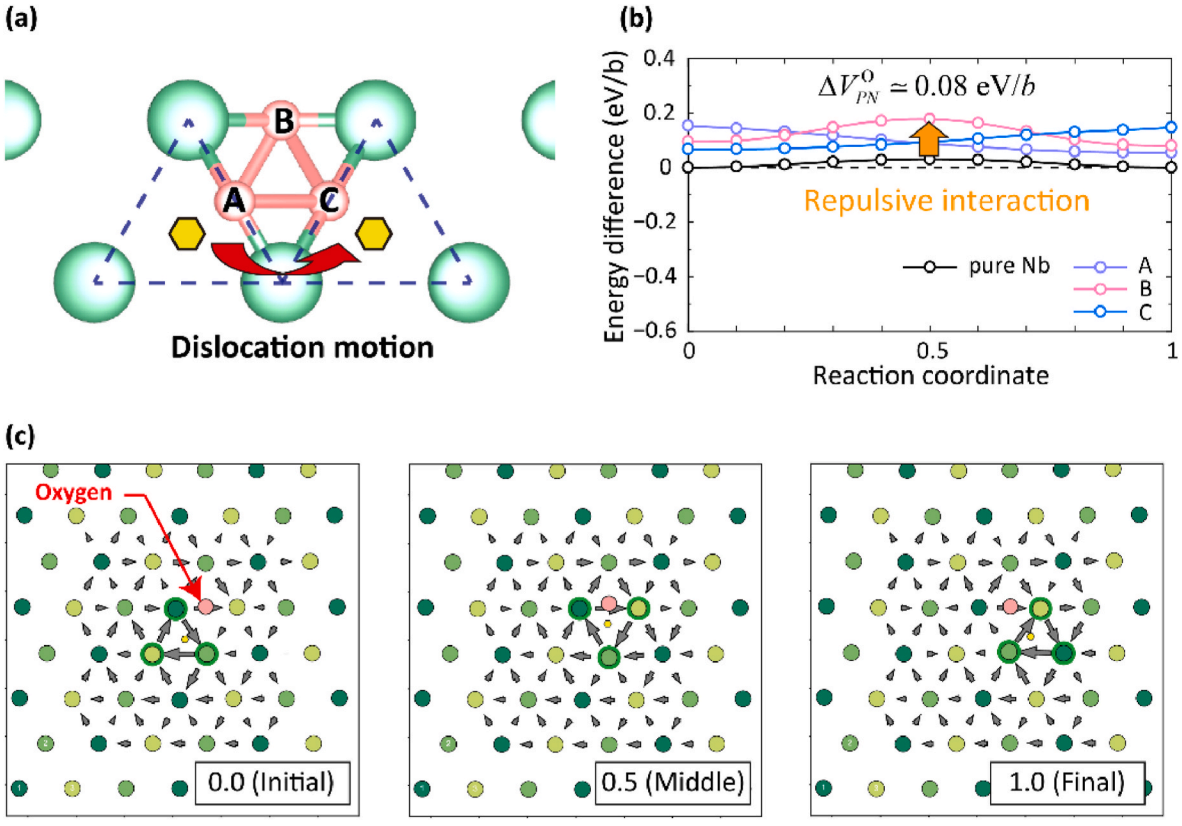

Fig. 5. Energy barrier for the dislocation motion around an oxygen interstitial. (a) Schematic of the atomic configuration for three interstitial sites shown in pink along the migration path of a dislocation core. (b) The change in energy during the motion of a screw dislocation around oxygen. (c) The change in the configuration of a dislocation core around an oxygen interstitial, as visualized by DD vectors. The oxygen is pushed slightly away when a screw dislocation approaches, as shown in 0.5 (Middle).

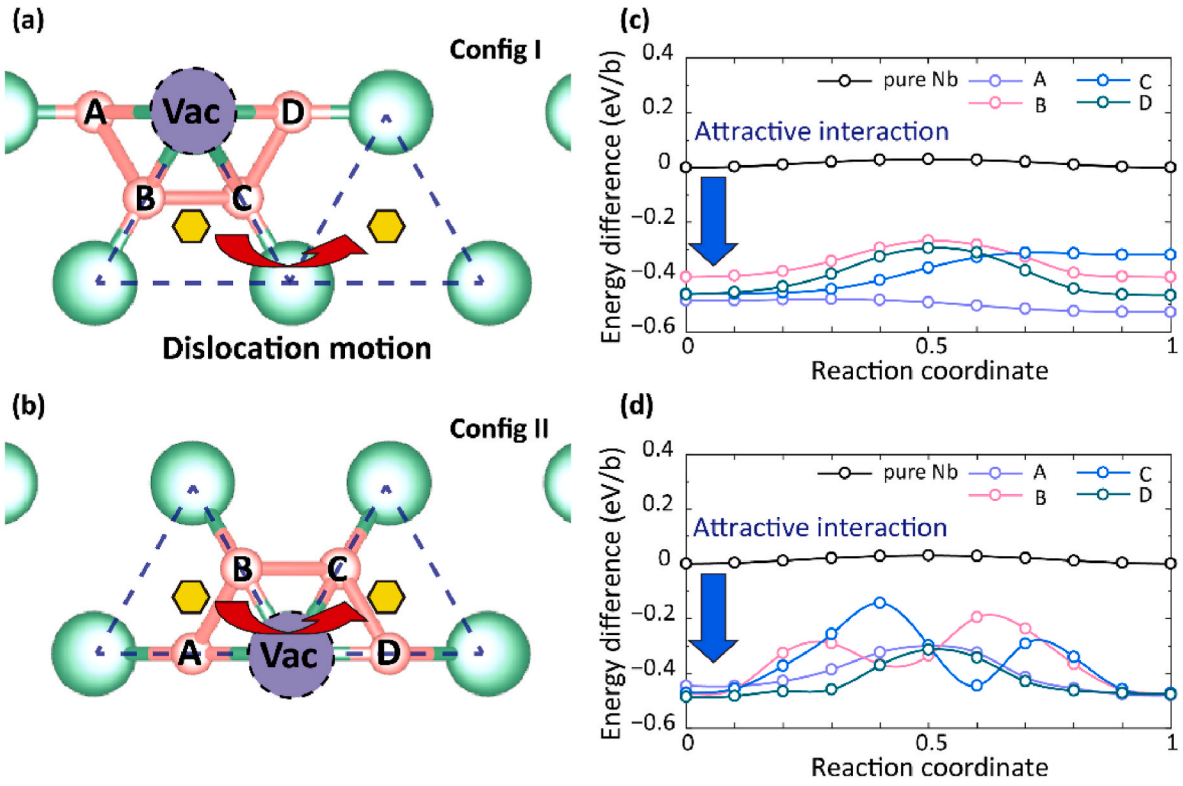

Fig. 6. Energy barrier for the dislocation motion around a vacancy–oxygen pair. Schematic of the atomic configuration of the dislocation core around the vacancy–oxygen pair of (a) Config I. and (b) Config II. (c) The change in the energy during the motion of a screw dislocation around the oxygen–vacancy pair corresponding to Config I. (d) Same as (c), but for Config II.

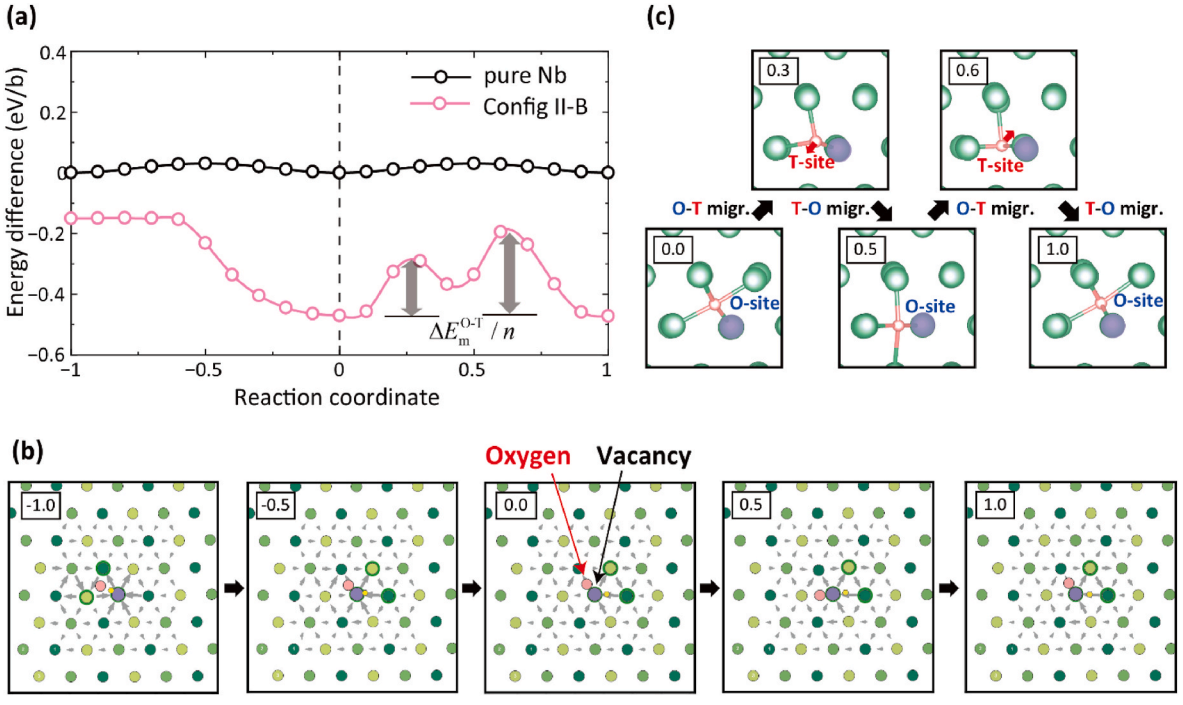

Fig. 7. Energy barrier associated with the positions of the dislocation core and the oxygen atom during dislocation motion around the vacancy–oxygen pair with Config II-B in Fig. 6. (a) The change in the energy during motion of the screw dislocation around the vacancy–oxygen pair. (b) The change in the configuration of the dislocation core around the vacancy–oxygen pair. (c) The change in the relative position of an oxygen interstitial during dislocation motion. The double-humped saddle-point configurations from 0 to 1 correspond to the tetrahedral site, indicating that octahedral–tetrahedral shuffling is necessary for dislocation motion.

alloys, where dislocations can move via a "mechanical shuffle" of the oxygen interstitial [45]. However, when only the oxygen interstitial is near the dislocation, the dislocation can only move if the oxygen shifts slightly in the Nb matrix, as mentioned above. By contrast, the dislocation motion across the vacancy–oxygen pair is strongly constrained because the oxygen is bound to the vacancy. The energy difference between the initial and saddle-point configurations is considerably higher for a vacancy–oxygen pair than a single lattice defect such as a vacancy and an oxygen interstitial. Interestingly, the double-humped energies of the saddle point correspond to the tetrahedral position, which increases the energy barrier for the dislocation motion; that is, octahedral–tetrahedral shuffling is induced by the vacancy-–oxygen–dislocation cooperative interaction. In this case, the energy barrier of the octahedral–tetrahedral transition $\Delta E_{\mathrm{m}}^{\mathrm{O-T}}$ of the oxygen atoms increases the Peierls barrier for the dislocation motion. In short, the Peierls barrier is inferred to be $\Delta V_{PN}^{\mathrm{Vac-O}} \simeq \Delta V_{PN}^{Vac} + \Delta E_{\mathrm{m}}^{\mathrm{O-T}} / n$, where ΔV_{PN}^{Vac} is the Peierls barrier around a vacancy and n is the length of the dislocation line normalized by the Burgers vector ($n = 3$ in the present model). As the energy of the octahedral–tetrahedral transition in the vicinity of the vacancy in the perfect crystal is 0.67 eV, $\Delta E_{\mathrm{m}}^{\mathrm{O-T}} / n$ is given as approximately 0.22 eV/b. This value is approximate because the energy $\Delta E_{\mathrm{m}}^{\mathrm{O-T}}$ should be different for the perfect crystal and the dislocation core. The energies of the two humps at the saddle point shown in Fig. 7 (a) are 0.18 and 0.27 eV/b, indicating that the hypothesis mentioned above correctly describes the significant increase in the Peierls barrier around the vacancy–oxygen pair. These results show that the vacancy–oxygen pair hinders local rearrangement of the dislocation core during the screw dislocation motion, presenting a strong obstacle to dislocation motion. In short, the vacancy–oxygen complex has a special effect on dislocation motion in addition to the attraction interaction between dislocation and a vacancy. Dislocations need to move by changing their slip plane rather than overcoming vacancy–oxygen obstacles. Thus, frequent cross-slip promotes cross-kink formation resultsing in significant strengthening in Nb–O alloys.

4. Summary

We investigated the fundamental process of dramatic oxygen-induced strengthening in niobium and revealed the underlying mechanism at the atomic level. In a previous study, we performed experiments, first-principles calculations, and molecular dynamics simulations to demonstrate that cross-kink nucleation enhances point-defect formation and damage accumulation, resulting in dramatic strain strengthening. DFT calculations showed that the formation of a vacancy–oxygen pair contributes considerably to the strengthening process, which induces an attractive interaction between the pair and a screw dislocation and increases the energy barrier for the dislocation motion [10]. In this study, we performed DFT calculations to determine whether this strengthening is unique only to oxygen and how the presence of a vacancy–oxygen pair results in a considerable increase in the energy barrier for the dislocation motion. C, N, and O interstitials show repulsive interactions with a screw dislocation. The N and O interstitials undergo an attractive interaction with a vacancy and the interaction between O and the vacancy (−0.80 eV) is stronger than that between N and the vacancy. These results support the formation of a stable oxygen–vacancy pair in the Nb matrix because of the attractive interaction between an oxygen interstitial and a vacancy [10]. The interaction energy between this vacancy–oxygen pair and a screw dislocation is approximately −0.5 eV and is dominated by the attractive interaction.

The attractive interactions caused by vacancies and vacancy–oxygen pairs undoubtedly affect dislocation motion; however, these interactions cannot solely explain dramatic strengthening. In addition to maintaining a stable oxygen distribution in the matrix, the presence of vacancy-–oxygen pairs increases the energy barrier for the motion of a screw dislocation more significantly than that of a single lattice defect. The mechanism of this increase in energy barrier was demonstrated using NEB simulations. As a result, the oxygen atom needs to move to the unstable tetrahedral interstitial site when the dislocation passes through a vacancy–oxygen pair; accordingly, octahedral–tetrahedral shuffling is necessary for the motion of a screw dislocation. In the real world, a screw dislocation tends to form cross-kink throught frequent cross-slip instead of overcoming such high-energy barrier vacancy–oxygen obstacle, which results in significant strengthening in Nb–O alloys.

Declaration of competing interest

The authors declare the following financial interests/personal relationships which may be considered as potential competing interests: Tomohito Tsuru reports financial support was provided by Japan Science and Technology Agency and Japan Society for the Promotion of Science. The other authors declare that they have no known competing financial interests or personal relationships that could have appeared to influence the work reported in this paper.

Acknowledgements

This study was supported by JST PRESTO (Grant No. JPMJPR1998), JST FOREST (Grant No. JPMJFR213P) and JSPS KAKENHI (Grant Nos. 18H05453, 22H01762). The simulation was performed on the large-scale parallel computer system of HPE SGI 8600 at JAEA. T.T. would like to acknowledge Prof. D. C. Chrzan for estimating the strengthening effect.

References

[1] Trinkle DR, Woodward C. The chemistry of deformation: how solutes soften pure metals. Science 2005;310:1665–7.
[2] Busby JT, Leonard KJ. Space fission reactor structural materials: choices past, present, and future. J Occup Med 2007;4:20–6.
[3] Tottle CR. The physical and mechanical properties of niobium. Inst Met 1957;85:375.
[4] Donoso JR, Reed-Hill RE. Slow strain-rate embrittlement of niobium by Oxygen. Metall Trans A 1976;7:961–5.
[5] Pint BA, DiStefano JR. The role of oxygen uptake and scale formation on the embrittlement of vanadium alloys. Oxid Metals 2005;63:33–55.
[6] Distefano JR, Chitwood LD. Oxidation and its effects on the mechanical properties of Nb-1Zr. J Nucl Mater 2001;295:42–8.
[7] El-Genk MS, Tournier JM. A review of refractory metal alloys and mechanically alloyed-oxide dispersion strengthened steels for space nuclear power systems. J Nucl Mater 2005;340:93–112.
[8] Leonard KJ, Busby JT, Zinkle SJ. Influence of thermal and radiation effects on microstructural and mechanical properties of Nb-1Zr. J Nucl Mater 2011;414:286–302.
[9] Liu G, Zhang GJ, Jiang F, Ding XD, Sun YJ, Sun J, Ma E. Nanostructured high-strength molybdenum alloys with unprecedented tensile ductility. Nat Mater 2013;12:344–50.
[10] Yang P-J, Li Q-J, Tsuru T, Ogata S, Zhang J-W, Sheng H-W, Shan Z-W, Sha G, Han W-Z, Li J, Ma E. Mechanism of hardening and damage initiation in oxygen embrittlement of body-centred-cubic niobium. Acta Mater 2019;168:331–42.
[11] Bilby BA. On the interactions of dislocations and solute atoms. Proc Phys Soc 1950;63:191–200.
[12] Medvedeva NI, YuN Gornostyrev, Freeman AJ. Solid solution softening and hardening in the group-V and group-VI bcc transition metals alloys: first principles calculations and atomistic modeling. Phys Rev B 2007;76:212104.
[13] Lu K, Lu L, Suresh S. Strengthening materials by engineering coherent internal boundaries at the nanoscale. Science 2009;324:349–52.
[14] Nie JF, Zhu YM, Liu JZ, Fang XY. Periodic segregation of solute atoms in fully coherent twin boundaries. Science 2013;340:957–60.
[15] Kuzmina M, Herbig M, Ponge D, Sandlobes S, Raabe D. Linear complexions: confined chemical and structural states at dislocations. Science 2015;349:1080–3.
[16] Rodney D, Ventelon L, Clouet E, Pizzagalli L, Willaime F. Ab initio modeling of dislocation core properties in metals and semiconductors. Acta Mater 2017;124:633–59.
[17] Zhao Y, Marian J. Direct prediction of the solute softening-to-hardening transition in WeRe alloys using stochastic simulations of screw dislocation motion. Model Simulat Mater Sci Eng 2018;26:045002.
[18] Ventelon L, Lüthi B, Clouet E, Proville L, Legrand B, Rodney D, Willaime F. Dislocation core reconstruction induced by carbon segregation in bcc iron. Phys Rev B 2015;91:220102 (R).
[19] Lüthi B, Ventelon L, Rodney D, Willaime F. Attractive interaction between interstitial solutes and screw dislocations in bcc iron from first principles. Comput Mater Sci 2018;148:21–6.

[20] Lüthi B, Ventelon L, Elsässer C, Rodney D, Willaime F. First principles investigation of carbon-screw dislocation interactions in body-centered cubic metals. Model Simulat Mater Sci Eng 2017;25:084001.
[21] Li Y-H, Zhou H-B, Gao F, Lu G, Lu G-H, Liu F. Hydrogen induced dislocation core reconstruction in bcc tungsten. Acta Mater 2022;226:117622.
[22] Itakura M, Kaburaki H, Yamaguchi M, Okita T. The effect of hydrogen atoms on the screw dislocation mobility in bcc iron: a first-principles study. Acta Mater 2013;61:6857–67.
[23] Daw MS. Elasticity effects in electronic structure calculations with periodic boundary conditions. Comput Mater Sci 2006;38:293–7.
[24] Zhang X-C, Cao S, Zhang L-J, Yang R, Hu Q-M. Unstable stacking fault energy and peierls stress for evaluating slip system competition in body-centered cubic metals. J Mater Res Technol 2023;22:3413–22.
[25] Tsuru T, Chrzan DC. Effect of solute atoms on dislocation motion in Mg: an electronic structure perspective. Sci Rep 2015;5:8793.
[26] Tsuru T, Wakeda M, Suzudo T, Itakura M, Ogata S. Anomalous solution softening by unique energy balance mediated by kink mechanism in tungsten-rhenium alloys. J Appl Phys 2020;127:025101.
[27] Cai W, Bulatov VV, Chang J, Li J, Yip S. Anisotropic elastic interactions of a periodic dislocation array. Phys Rev Lett 2001;86:5727–30.
[28] Cai W, Bulatov VV, Chang J, Li J, Yip S. Periodic image effects in dislocation modelling. Philos Mag A 2003;83:539–67.
[29] Clouet E, Ventelon L, Willaime F. Dislocation core energies and core fields from first principles. Phys Rev Lett 2009;102:055502.
[30] Clouet E, Ventelon L, Willaime F. Dislocation core field. II. Screw dislocation in iron. Phys Rev B 2011;84:224107.
[31] Dezerald L, Proville L, Ventelon L, Willaime F, Rodney D. First-principles prediction of kink-pair activation enthalpy on screw dislocations in bcc transition metals: V, Nb, Ta, Mo, W, and Fe. Phys Rev B 2015;91:094105.
[32] Clouet E, Bienvenu B, Dezerald L, Rodney D. Screw dislocations in BCC transition metals: from ab initio modeling to yield criterion. Compt Rendus Phys 2021;22.83–75.
[33] Clouet E, Varvenne C, Jourdan T. Elastic modeling of point-defects and their interaction. Comput Mater Sci 2018;147:49–63.
[34] Kresse G, Hafner J. Ab initio molecular dynamics for liquid metals. Phys Rev B 1993;47:558–61.
[35] Kresse G, Furthmuller J. Efficient iterative schemes for ab initio total-energy calculations using a plane-wave basis set. Phys Rev B 1996;54:11169–86.
[36] Perdew JP, Chevary JA, Vosko SH, Jackson KA, Pederson MR, Singh DJ, Fiolhais C. Atoms, molecules, solids, and surfaces: applications of the generalized gradient approximation for exchange and correlation. Phys Rev B 1992;46:6671–87.
[37] Monkhorst HJ, Pack JD. Special points for Brillouin-zone integrations. Phys Rev B 1976;13:5188–92.
[38] Henkelman G, Uberuaga BP, Jónsson H. A climbing image nudged elastic band method for finding saddle points and minimum energy paths. J Chem Phys 2000;113:9901–4.
[39] Momma K, Izumi F. VESTA 3 for three-dimensional visualization of crystal, volumetric and morphology data. J Appl Crystallogr 2011;44:1272–6.
[40] Vítek V, Perrin RC, Bowen DK. The core structure of ½(111) screw dislocations in b.c.c. crystals. Philos Mag A 1970;21:1049–73.
[41] Nye JF. Some geometrical relations in dislocated crystals. Acta Metall 1953;1:153–62.
[42] Wenskat M, et al. Vacancy dynamics in niobium and its native oxides and their potential implications for quantum computing and superconducting accelerators. Phys Rev B 2022;106:094516.
[43] Wenskat M, et al. Vacancy-hydrogen interaction in niobium during low-temperature baking. Sci Rep 2020;10:8300.
[44] Itakura M, Kaburaki H, Yamaguchi M. First-principles study on the mobility of screw dislocations in bcc iron. Acta Mater 2012;60:3698–710.
[45] Yu Q, Qi L, Tsuru T, Traylor R, Rugg D, Morris Jr JW, Asta M, Chrzan DC, Minor AM. Origin of dramatic oxygen solute strengthening effect in titanium. Science 2015;347:635–9.